Preferred citation: J. Salmela and M. Kataja. Floc rupture and re-flocculation in turbulent shear flow. In **Advances in Paper Science and Technology**, *Trans. of the XIIIth Fund. Res. Symp. Cambridge, 2005*, (S.J. I'Anson, ed.), pp 35–50, FRC, Manchester, 2018. DOI: 10.15376/frc.2005.1.35.

FLOC RUPTURE AND RE-FLOCCULATION IN TURBULENT SHEAR FLOW

J. Salmela and M. Kataja

VTT Processes, Multiphase Flows, Po.Box 1603, 40101 Jyvaskyla, Finland

ABSTRACT

The dynamics of fibre suspension flow, especially breakup and reformation of fibre flocs in a closed channel flow past a forward facing step was studied experimentally using fast CCD camera imaging and image analysis techniques that allow for simultaneous measurement of floc size and turbulent flow field of fibres. The recirculation eddy downstream of the expansion step was found to exists only if the step height exceeds mean fibre length. When existing, the behavior of the eddy is similar to that of Newtonian fluid flows. Experimental correlations between floc size and turbulent flow quantities were found indicating that the ratio of the minimum floc size found at the end of the recirculation region and the floc size upstream of the step is strongly correlated with the size of the largest scales of the turbulent field and less directly with the total turbulent intensity of the flow immediately after the step. In addition, an approximate power law scaling behavior of the floc size with the turbulent intensity was found within the decaying turbulence region downstream of the recirculation eddy.

1 INTRODUCTION

In a typical consistency range of fibre suspensions used in paper-making, fibres have a strong tendency to form aggregates the properties of which depend on flow conditions (see refs. [1, 2, 3, 4]). At low shear, the fibres may form large inhomogeneous (flocculated) networks with properties reminiscent of a soft porous solid material. At turbulent high shear conditions, the network is broken into smaller flocs and the suspension becomes 'fluidized'. In many processes of paper-making it is necessary to bring the suspension in such a fluidized state in order *e.g.* to facilitate flow, to homogenize the suspension or to enhance mixing. Within the forming process in particular, control of the degree of fluidization, *i.e.* the floc size distribution, and even of the properties of individual flocs is sought. In practice, the flocculated state of the suspension can, to some extent, be affected by controlling the intensity and quality of the turbulence within the flow. This, in turn, can be attained *e.g.* by regulated mixing or by local losses induced by a particular geometry of the flow channel. The primary problem in such a control is that, in spite of an extensive number of studies on this topic (see refs. [5, 6, 7, 8, 9, 10, 11]), very little is known of the actual dynamics of turbulence of fibre suspensions and of interactions between fluid turbulence and fibre network.

The primary goal of this study was to gain new experimental information on the behavior of turbulent flow of wood fibre suspensions past a sudden axisymmterical pipe expansion. We analyze the effects of fibres on the length of the recirculation eddy after the expansion step, and correlate floc break-up and reflocculation with the properties of the turbulent flow field in a straight tube section downstream of the expansion step. The experiments were carried out utilizing two measurement techniques developed earlier, namely floc size analysis [12, 7, 9] and a novel local fibre phase velocity field analysis. Both measurements are based on fast CCD camera imaging and on an appropriate image analysis techniques.

2 EXPERIMENTAL SET-UP AND METHODS

Experiments were carried out on a flow line composed of a 1 m^3 tank, a centrifugal pump and a flow loop of plastic pipe with 40 mm inner diameter (see Figure 1 (a)). The acrylic cylindrical test channels mounted on the flow line included a sudden forward facing step as shown in Figure 1 (b).

The diameter of the constriction tube upstream of the step was varied between 12 and 20 mm. The length of the constriction tube was 500 mm. For

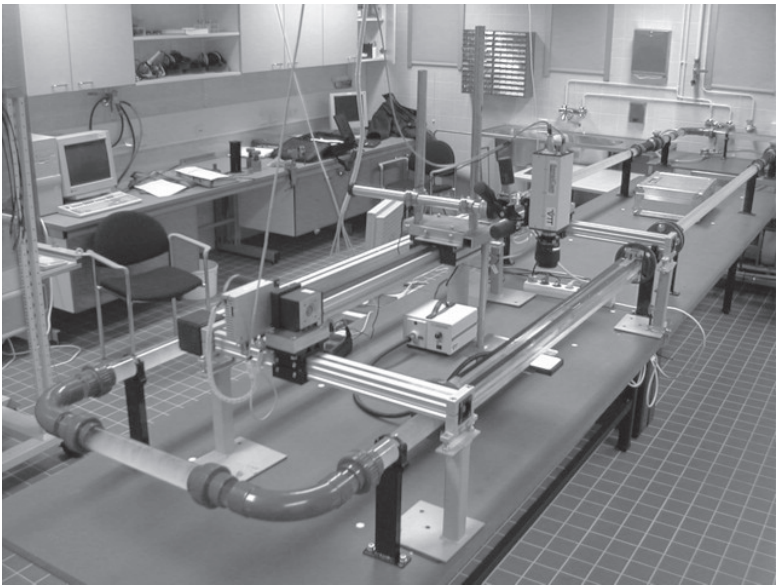

(a)

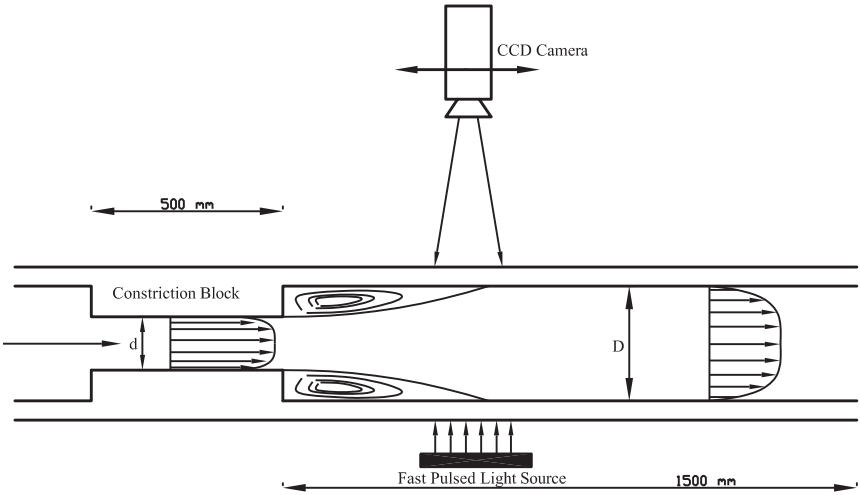

(b)

Figure 1 (a) Overview of the laboratory flow line used in the experiments. (b) Schematic illustration of the test tube section and the experimental set-up.

Table 1 Dimensions of the flow geometries together with the measured values of head loss coefficient C_L over the step expansion. Here, d and D are the diameter of the constriction and downstream tube sections, respectively, and $\triangle h$ is the corresponding expansion step height.

d	$D = 26$ mm		$D = 21$ mm	
[mm]	$\triangle h$ *[mm]*	C_L	$\triangle h$ *[mm]*	C_L
12.0	7.0	0.62	–	–
14.0	6.0	0.52	3.5	0.31
16.0	5.0	0.39	2.5	0.18
18.0	4.0	0.27	–	–
20.0	3.0	0.16	–	–

the downstream tube section of length 1500 mm, two different diameters, 21 mm and 26 mm, were used. The combinations of the test tube diameters used in the experiment are given in Table 1. Also given are the values of head loss coefficient of the sudden expansion for the used dimensions. These values are measured for water, but apply very accurately for all the five different fibre suspensions used in the experiments (see below).

Details of the flow field and evolution of the floc size in the tube section downstream of the constriction tube was measured using a fast double-exposure CCD camera (PCO Sensicam) mounted above the test channel. The channel was transilluminated from below by a pulsed plane light source. The flow rate, position of the light source and camera, exposure and lighting synchronization were fully computer-controlled. Typically, images were taken at 20 positions along the test tube with 200 double-exposures collected at each position. The images were corrected for uneven illumination and the distribution of floc size was found using median thresholding method described in detail in refs. [12] and [9]. Typical image width was 35 mm and pixel size 0.13 mm. The new fast pulsed plane light source, specifically designed for the present experiment, comprised of an array of 40 ultra-bright white light emitting diodes evenly spaced on a close-packing lattice. The luminance intensity of each LED is 10 000 mcd and the total size of the LED array is 50 × 27 mm. The minimum pulse duration is 15 μs and the maximum pulse repetition frequency is 67 kHz. The device enables fast and accurately timed double exposure and thereby, simultaneous measurement of floc size and fibre phase displacement fields. The two-dimensional displacement field between the two consecutive images and consequently, the local instantaneous velocity field was determined using a specific cross-correlation and

optimization algorithm. From this information it is then possible to calculate flow field properties such as flow rate, mean velocity profile, fibre phase streamlines and even turbulence properties such as turbulent intensity, Reynolds stress and dissipation. Notice, however, that the correlation method used here is originally developed for, and most directly applicable in two-dimensional flows. In the present three-dimensional flow condition the velocity field obtained by this method corresponds to some extent unspecified average over the vertical direction through the channel. The absolute values of velocity may therefore not be accurate in some parts of a three dimensional flow geometry. It appears, however, that in the present case where the step producing the three dimensional mean flow pattern is not very high, the measured flow field can indeed be used to gain reliable information on cross features of the flow. Furthermore, the turbulence quantities calculated from a large number of measured instantaneous flow fields appear to provide a useful qualitative measure of the local fibre phase velocity fluctuations in the present flow conditions, as independently verified by other methods such as pulsed ultrasound-Doppler anemometry. We emphasize however that so far, no effort has been made to quantitatively validate the present method for turbulence measurements.

In addition to measurements based on image analysis, overall loss in the constriction tube, over the expansion step and in the downstream tube were found by differential pressure measurements.

A series of experiments were carried out using two different pulps, namely Scandinavian birch and pine. Both pulps were unbeaten and contained no fillers or added chemicals. In addition, three different fibre length fractions of pine were used. Fractioning was done using pressure screen as gently as possible to minimize beating of fibres. The resulting fibre length distribution of original pulps and each fraction are shown in Figure 2. The relevant fibre properties of the suspensions are summarized in Table 2.

All experiments were done at 1.0% consistency. Before each measurement, the suspension was circulated in the flow loop for 30 minutes in order to allow for suspension to homogenize. Microscopic examination of fibres, flock size analysis and freeness tests were used to verify that fibre properties remained constant during measurement period. Two different flow rates, 1.0 l/s and 2.0 l/s were used. With the dimensions given in Table 1 the mean flow velocity in the constriction tube was thus varied between 3.2 and 17.8 m/s, corresponding to values of Reynolds number between $0.6 \cdot 10^5$ and $2.1 \cdot 10^5$ (calculated using viscosity of water).

The length of the recirculation eddy was defined as the distance from the expansion step to the stagnation point found at channel wall. The stagnation point and the maximum mean recirculation velocity within the eddy were

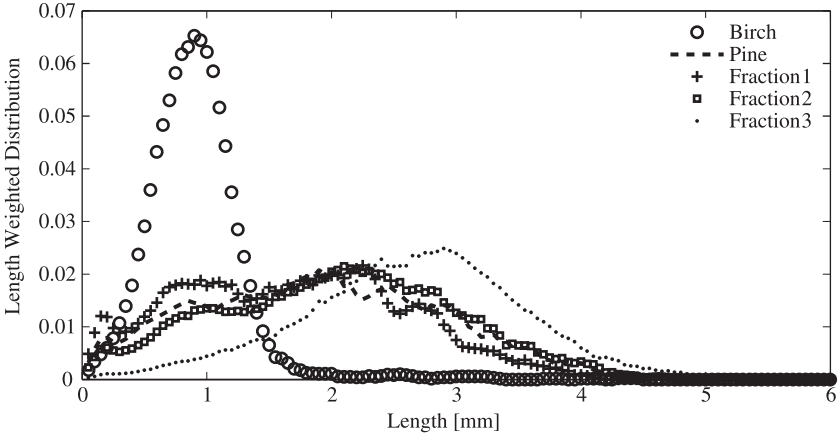

Figure 2 Fibre length distribution for the pulps used.

Table 2 Basic fibre properties of used suspensions. The crowding number given in the last column is defined as $N_{cf} = 5C_m l_f^2/w$, where $C_m = 1\%$ is the fibre mass concentration.

Pulp	*Average Fibre Length* l_f*[mm]*	*Average Fibre Diam.* d_f*[μm]*	*Fibre Coarseness* w*[mg/m]*	*Crowding number* N_{cf}
Birch	0.92	16.7	0.114	37
Pine	2.05	22.0	0.206	102
Pine / fraction 1	1.71	19.8	0.198	73
Pine / fraction 2	2.07	22.9	0.209	102
Pine / fraction 3	2.66	30.5	0.220	160

determined by analyzing the long time mean flow field obtained as an average of 200 individual flow patterns.

Median thresholded images were used to calculate the dimensionless mean floc volume,

$$V_f^* = \frac{< L_x >< L_y >^2}{l_f^3}, \tag{1}$$

at each imaging location along the test tube. Here, l_f is the length weighted mean fibre length, $< L_x >$ and $< L_y >$ are the length weighted mean floc dimensions in flow direction and cross direction respectively [7, 12], and <> denotes average over the image area and over the 200 exposures taken at each imaging position. Using the measured floc volume before the expansion V^*_0, and the minimum floc volume after the expansion V^*_{min}, we define the Floc Rupture Ratio (FRR)

$$FRR = \frac{V^*_{min}}{V^*_0} \tag{2}$$

which characterizes the efficiency of floc breakage due to the turbulent field induced by the step expansion. Finally, the turbulent intensity

$$I_t = \frac{< u'u' + v'v' >}{< u >^2} \tag{3}$$

was calculated at each imaging location. Here u' and v' are the fluctuation components of the flow velocity in longitudinal and transverse directions, respectively, and $< u >$ is the mean velocity in the channel.

3 RESULTS

Figure 3 (a) shows an example of a result obtained by the simultaneous floc and flow field measurement based on image analysis. The image shown is for a flow of pine suspension in 26 mm tube, at a location 450 mm downstream of the expansion step of height 6 mm. The flow rate is 2.0 l/s corresponding to a mean velocity of ~3.8 m/s. The background image shows a single illumination corrected snapshot of the suspension. The domains identified as 'flocs' by median threshoding method are indicated by enhanced boundaries. The horizontal and vertical floc size distributions are determined from a number of such images as floc area segment length distributions in the two orthogonal directions. The arrows indicate an instantaneous flow field found by the correlation analysis of a single pair of double exposure images at the same location. As indicated by the arrow pattern, the flow is well developed with a characteristic plug-shaped velocity profile at this position and fluctuations are already quite small. The corresponding turbulent velocity field is determined locally as deviation of these instantaneous velocity vectors from the mean velocity vectors found by averaging over 200 similar image pairs. Figure

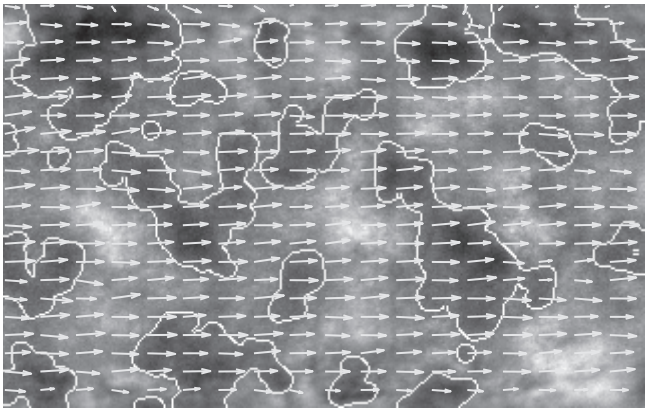

(a)

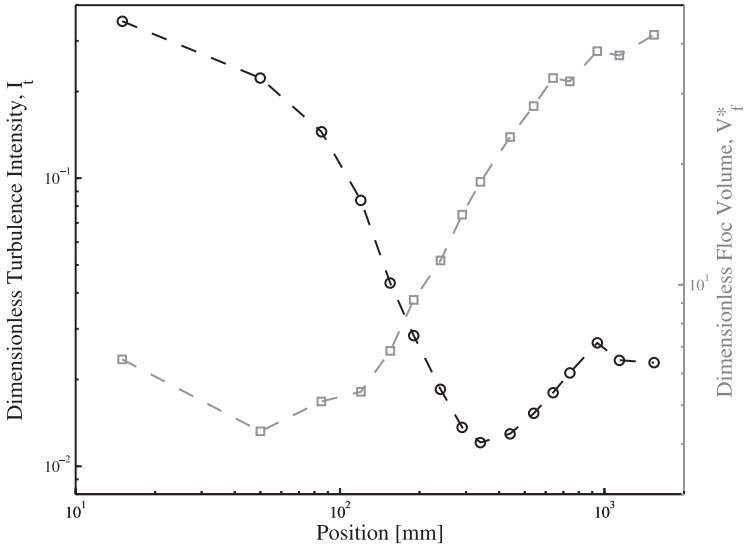

(b)

Figure 3 (a) Instantaneous velocity field and floc image taken at a location 450 mm downstream of the expansion step. The background layer shows a single illumination corrected gray scale image with floc boundaries enhanced. (b) The measured dimensionless floc volume (□) and turbulent intensity (○) as a function of position after the expansion step. All values are obtained by averaging over the entire image area and over 200 exposures.

3 (b) shows the measured mean turbulent intensity and mean floc size at each imaging location along the tube downstream of the expansion. The flow condition, tube geometry and suspension are the same as for Figure 3 (a). Three different domains of flow downstream of the expansion step can be identified. First, there is the recirculation region which in this case typically extends to ~45 mm downstream from the step (see below). In this region, the measured turbulence intensity is high and the floc size degreases. The minimum floc size is achieved at the end of recirculation region. The second region is that of decaying turbulence, where the measured turbulent intensity decreases and floc size increases. This domain covers the distance ~300 mm downstream of the recirculation region. Beyond that point, the measured turbulent intensity slightly increases while the floc size continues to increase as well. This region is most likely associated with the still evolving flow profile and establishing of the stationary turbulence profile of fully developed flow. Notice, that the present measuring method is more sensitive to flow near the tube wall. The observed increase of turbulent intensity may thus be affected by increased intensity especially within the developing turbulent boundary layer. Based on the present results, it is not clear whether any fully developed region is achieved within the 1500 mm length of the downstream channels used here. In most cases, the mean flow profile and the turbulent intensity seem to saturate towards the end of the channel. Instead, the measured floc size mostly seems to keep evolving up to the very end of the channel.

3.1 Recirculation length

A characteristic feature of a flow over a forward facing step is the existence of a recirculation eddy, a phenomenon that is well known for flows of Newtonian fluids. In order to identify the possible qualitative differences between flows of Newtonian fluids and fibre suspensions past a sudden expansion, we first apply the image analysis method in measuring the length of the recirculation eddy in the present flow geometries. Figure 4 shows an example of a mean flow field of fibre phase after the sudden expansion in a cylindrical tube as measured using the double exposure correlation method. The flow reattachment location marking the length of the recirculation eddy is clearly identifiable near the point $x/h_s = 6$.

The measured values of the recirculation eddy length are given in Table 3 for various step heights and suspensions used. Figure 5 summarizes the same data in a dimensionless form where the eddy length is scaled by the step size, and the step size by the mean fibre length.

In the cases where the step height h_s is larger than the mean fibre length l_f, a

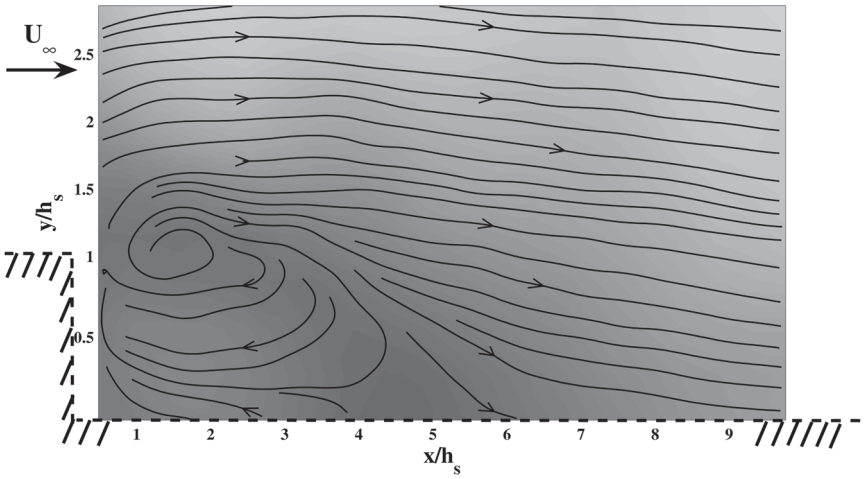

Figure 4 Measured streamlines of fibre phase after sudden expansion for 1.0% birch suspension. Background color indicates the mean fibre phase speed (darker color for lower speed). Dashed line indicates channel wall position at the center plane of the cylindrical tube.

Table 3 Measured recirculation length for different fibre types and values of step height. For pine and birch, results for flow rates 1.0 l/s and 2.0 l/s are given. For the three fibre length fractions of pine, the results are given for flow rate 2.0 l/s only.

Step Height [mm]	***Recirculation length [mm]***				
	Birch 1.0/2.0 l/s	*Pine 1.0/2.0 l/s*	*Pine/Fract. 1*	*Pine/Fract. 2*	*Pine/Fract. 3*
2.5	13.2/–	0.00/–	14.4	0.00	0.00
3.0	14.4/15.0	4.8/0.00	–	–	–
3.5	–/–	–/–	18.0	22.8	0.00
4.0	24.0/25.0	22.8/23.0	–	–	–
5.0	32.4/36.0	30.0/42.0	31.2	28.8	–
6.0	45.6/47.0	44.4/51.0	42.0	42.0	39.6
7.0	58.8/70.0	57.6/66.0	–	–	–

recirculation eddy with characteristics similar to that of Newtonian fluids appears. Notice that for fully turbulent flow of Newtonian fluids, typical values of the dimensionless eddy length L_e/h_s vary between 5 and 8 and the maximum backward velocity found in the recirculation eddy is ~ $-0.22U$,

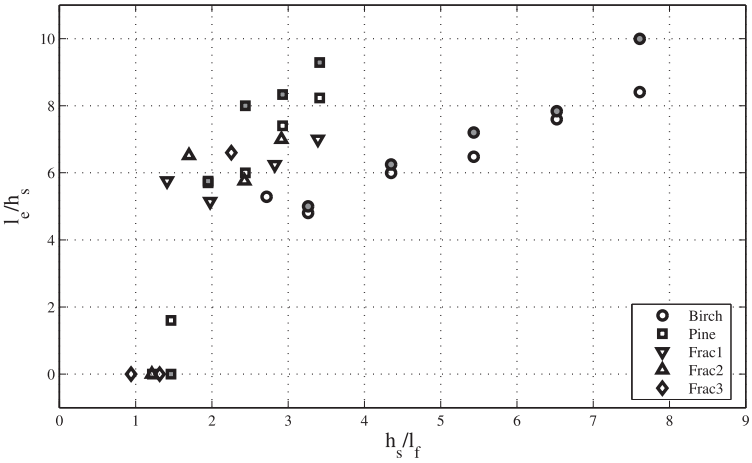

Figure 5 The measured dimensionless length of the standing vortex after sudden expansion as a function of dimensionless step height (open symbols for 1.0 l/s and filled symbols for 2.0 l/s). Here, l_e is the length of the vortex, h_s is the step height and l_f is the mean fibre length.

where U is the mean velocity upstream of the step [13, 14, 15]. In the current experiments we find most values of L_e/h_s in the range from 5 to 9, and the maximum recirculation velocity ~ $-0.20U$. These values apply for all types of suspension measured. The results thus indicate that in highly turbulent flow conditions, and in geometries where the recirculation eddy exists, *i.e.* the step height is large enough, the behavior of the recirculation eddy is very similar to that of Newtonian fluid for all the five suspensions studied here. If, instead, the step height is comparable to or less than the mean fibre length, no recirculation eddy is observed. It is evident that fibre length sets the lower limit for the eddy size scale of the fibre phase flow.

3.2 Floc rupture

In general, one may expect the efficiency by which the turbulent flow field is able to disintegrate flocs, be dependent on the turbulent energy spectrum of the flow. Here, wee seek to correlate the floc rupture ratio FRR, defined by Equation (2), with measured quantities characterizing the overall turbulent intensity and the typical turbulent scales present in the recirculation zone. To this end, in Figures 6 (a) and (b) we have plotted the floc rupture ratio as a function of head loss over the expansion and of the dimensionless step

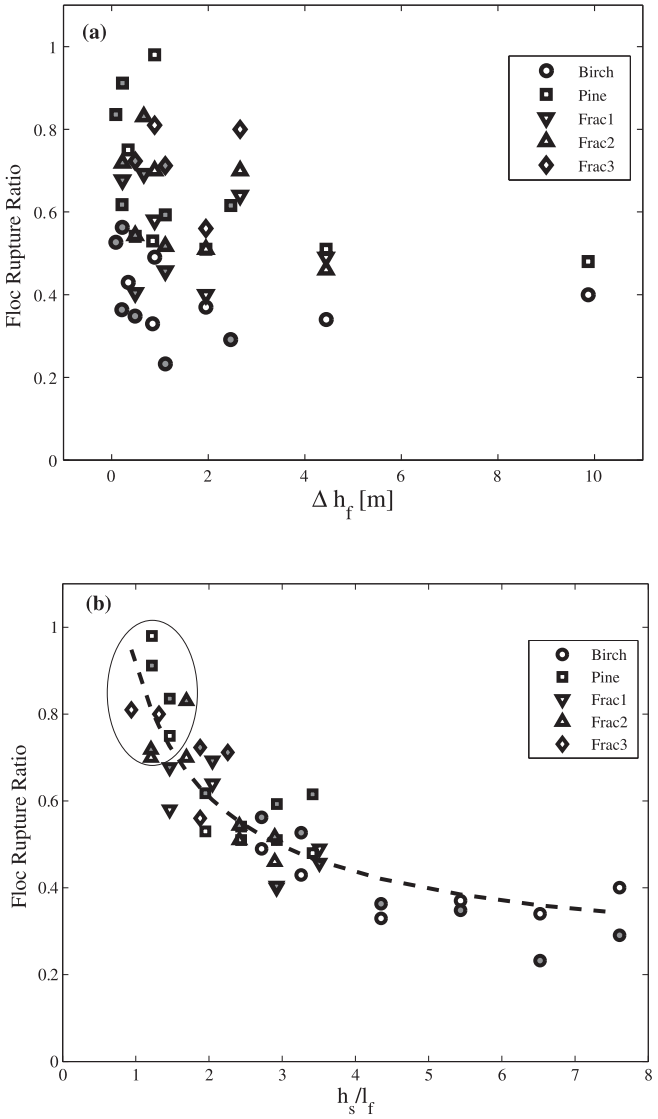

Figure 6 (a) Floc Rupture Ratio for different fibre types and flow rates 1.0 *l*/*s* (filled symbols) and 2.0 *l*/*s* (open symbols) as a function of head loss Δh_f. (b) Floc rupture ratio as a function of relative step height. Dashed line shows the result of a fit by a function given in Equation (4). The symbols enclosed by a line represent cases where no recirculation eddy was observed.

height, respectively. Notice, that the step height h_s determines the largest scales present in the recirculation eddy region, whereas loss characterizes the total turbulent energy and the smallest (dissipative) scales. Somewhat surprisingly, it appears that no reasonable correlation is found between the measured values of FRR and head loss in the present experiments. Instead, clear data collapse occurs when FRR is presented as a function of the ratio of the step size to fibre length, as shown in Figure 6 (b). Furthermore, the data including all measured cases with varying flow rate, step size and fibre type can be fitted with a single function of the form

$$FRR = a\left(\frac{h_s}{l_f}\right)^{-b} + c, \tag{4}$$

with the parameter values $a = 0.7$, $b = 0.8$ and $c = 0.2$. This finding can be compared with the previous result by Karema *et. al.*, [9], who found a power law correlation between the dimensionless minimum floc size and head loss. Although not shown, the present data supports that result. The absolute minimum floc size is, however, affected by properties of incoming flow whereas FRR more directly reflects the effect of the step alone. Another difference is that Karema's experiments were done using constant crowding number by varying consistency of different fibre types, while the current study is done at a constant consistency and varying crowding number. The result summarized in Figure 6 (b) and in Equation (4) seems to imply that at least in the conditions of this particulate experiment, the floc rupture ratio is more directly related with the largest scales present in the turbulent field than with the total turbulent intensity or with dissipative scales.

3.3 Reflocculation in the decaying turbulence region

Finally, we made an effort to correlate the measured values of floc volume and turbulent intensity within the region of decaying turbulence. At flow rate 2.0 l/s this region extends approximately 300 mm downstream of the recirculation region, irrespectively of the step size and type of suspension. Figure 7 shows the measured dimensionless floc size as a function of the turbulent intensity within the decaying turbulence region for all step sizes and suspensions used at 2.0 l/s flow rate. The data indicates an approximate scaling of the dimensionless floc volume as –2/3 power of the measured turbulent intensity. In this case, however, only moderate data collapse is found. Furthermore, no obvious scaling of variables were found that would have significantly improved the result. This is not very surprising, though, since existence

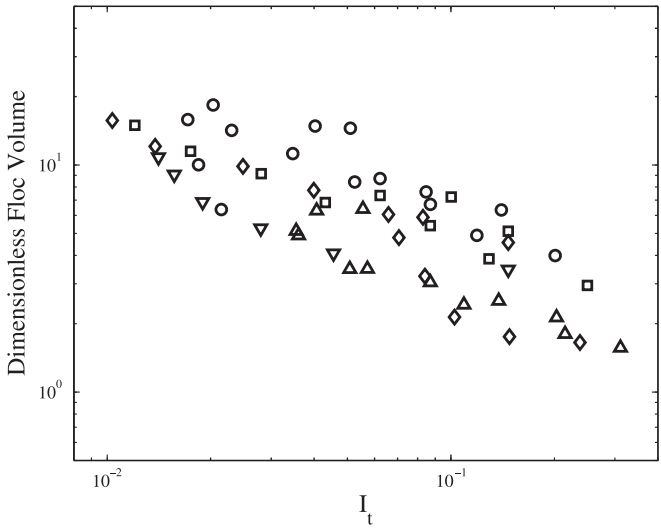

Figure 7 The dimensionless floc volume as a function of turbulent intensity in the decaying turbulence region at 2.0 l/s flow rate (○ birch, □ pine, ▽ Fraction 1, △ Fraction 2 and ◇ Fraction 3).

of such general direct correlation between floc size and turbulent intensity would indicate that reflocculation in decaying turbulent field is a quasi-stationary process, *i.e.* that the floc size at each instant of time acquires the equilibrium value particular to the momentary value of turbulent intensity. Instead, reflocculation may more likely be described as a relaxation process where the turbulent intensity defines the rate of change of the floc size. Further study of this interesting problem as well as the behavior of the floc size in the developing flow region after the decaying turbulence region is left for a future work.

4 DISCUSSION

We have used floc size analysis and two-dimensional fibre phase velocity field analysis to experimentally study the behavior of fibre suspension flow in a cylindrically symmetric channel with a sudden expansion step. The two methods are based on fast CCD camera double exposure imaging with appropriate illumination and image analysis techniques. Same set of images are used for analysis of both the floc size and the velocity field. The results reveal three dynamically different regions in the flow downstream of the step

expansion, namely recirculation region, decaying turbulence region and developing pipe flow region. No clear fully developed flow was achieved within the available test channel length. The behavior of the recirculation eddy observed at step heights exceeding the mean fibre length was similar to that found for simple Newtonian fluids. For step heights comparable or less than the mean fibre size, no recirculation eddy was formed. The floc rupture ratio (FRR), defined as the ratio of the minimum floc size found at the end of the recirculation region and the floc size upstream of the step, was found to be correlated with the ratio of step size to fibre length, whereas no correlation between FRR and the loss induced by the expansion step was found. This indicates that, in the present flow conditions, FRR is more directly dependent on the size of the largest scales of the turbulent field than on the overall turbulent intensity of the flow immediately after the step. Finally, an approximate power law scaling behavior of the floc size with the turbulent intensity was obtained in the decaying turbulence region. In this case, however, the observed correlation between the floc size and turbulent intensity with different channel geometries and suspensions was not very strong. More detailed analysis of the floc evolution data in the decaying turbulence and developing flow regions is left for a future work.

References

1. Duffy, G., E. R. M. K. and Norman, B., "Hydrodynamics of papermaking fibres in water suspension," *6th Fundamental Research Symposium*, Pulp and Paper Fundamental research Society, April 1977.
2. Kerekes, R. J., S. R. M. and Tam Doo, P. A., "The flocculation of pulp fibres," *Transactions of the 8th Symposium*, Vol. 1, 1985, pp. 265–310.
3. Hourani, M. J., "Fiber flocculation in pulp suspension flow. Part 1: Theoretical model," *Tappi J.*, Vol. 115–118, 1988.
4. Hourani, M. J., "Fiber flocculation in pulp suspension flow. Part 2: Experimental results," *Tappi J.*, Vol. 186–188, 1988.
5. Norman, B., "Turbulence and Flocculation Measurements In Fibre Suspensions," *International Symposium on Papermachine Headboxes (Invited lecture)*, McGill University, June 3–5 1979, Montreal.
6. Kerekes, R. J., "Pulp Flocculation in Decaying Turbulence," *J. Pulp Pap.Sci*, Vol. 7, 1983, pp. 86–91.
7. Karema, H., K. M., "Transient Fluidisation of Fibre Suspension in Straight Channel Flow," *Proceedings of the TAPPI International Paper Physics Conference*, Sept. 1999.
8. Holm, R., *Fluid mechanics of fibre suspensions related to papermaking*, Doctoral thesis, Royal Institute of Technology (KTH), 2005, Stockholm, Sweden.
9. Karema H., Salmela J., T. M., "Predicion of paper formation by fluidisation and

reflocculation experiments," *12th Fundamental Research Symposium*, Sept. 2001, pp. 559–589.
10. Bonano, E. J., A., "Study of floc breakup and formation in flowing concentrated fiber suspensions," *Int. J. Multiphase Flow*, Vol. 10, No. 5, 1984, pp. 623–637.
11. Steen, M., "Modeling fibre flocculation in turbulent flows: a numerical study," *Tappi J.*, Vol. 74, No. 9, 1991, pp. 175–181.
12. Kellomäki M., Karema H., K. M., "Fiber flocculation measurement in pipe flow by digital image analysis," *Proceedings of the TAPPI International Paper Physics Conference*, Sept. 1999, pp. 461–463.
13. Poole R.J., E. M., "Turbulent flow of viscoelastic liquids through an axisymmetric sudden expansion," *Journal Of Non-Newtonian Fluid Mechanics*, Vol. 117, 2004, pp. 25–46.
14. Poole R.J., E. M., "Turbulent Flow of Non-Newtonian Liquids over a Backward-Fasing Step Part 1. A Thixotropic and shear-Thinning liquids," *Journal of Non-Newtonian Fluid Mechanics*, Vol. 109, 2003, pp. 177–191.
15. Poole, R.J., E. M., "Turbulent Flow of Non-Newtonian Liquids over a Backward-Fasing Step Part 2. A Viscoelastic and shear-Thinning liquids," *Journal Of Non-Newtonian Fluid Mechanics*, Vol. 109, 2003, pp. 193–230.

Transcription of Discussion

FLOC RUPTURE AND RE-FLOCCULATION IN TURBULENT SHEAR FLOW

J. Salmela and M. Kataja

VTT Processes, Multiphase Flows, P.O. Box 1603, 40101 Jyvaskyla, Finland

Wolfgang Bauer Graz University of Technology

You have built what is, more or less, a two-dimensional model of a three-dimensional flow field. Is there not any problem with this? Do you really get a true representation?

Juha Salmela

Very good question. We have not really developed a model. The problem with this method is that the experimental setup is designed for 2-D flows, but we just decided to test it on practical applications, like the turbulence generator, and it turned out that the method gave us good results. I am not saying that we can use our results to obtain absolutely the correct turbulence level, but, when we use the same method to study these effects, we can gain at least some understanding and relative information. Things like stagnation point and recirculation length are very accurately defined. I can say that our method works and gives accurate information, but this is still a relatively new method for us. So, I am not saying that turbulence intensity values are exactly correct but I am trying to show that we can get an idea of the phenomena behind these things.

Wolfgang Bauer

Have you validated against another method like anemometry or something similar?

Juha Salmela

No, not yet. As I said our long-term goal is to validate existing floc and multiphase flow models, and also to develop new models. I am sure that we will do some more experiments with 2-D geometries just to make sure that we get accurate information with this method.

Daniel Söderberg STFI-Packforsk AB

I have a question regarding the entrance to this constriction. Could you comment on the influence the entrance to the constriction zone will have on flocculation, because you have very different elongational strain?

Juha Salmela

Again, a really good question. At this point, the only comment I can make is that the constriction in this case is so long that we have reached saturation size. So, we have a fully developed velocity profile and saturation in the floc size. Actually, the next thing I plan to do is to find an answer to your question. So, hopefully, in six months I will be able to answer that.

Theo van de Ven McGill University

You show how the floc volume changes, but can you also say something about other parameters of the flocculation process like how much of the fibre is in the form of flocs? Can you tell something from your measurements about the mechanism of fibre floc break-up? Does a floc break up into pieces or do individual fibres leave the floc? Can you say anything about these things from your observations?

Juha Salmela

Actually, I cannot. The spectrum of the break-up is something that we did not actually have time to look into, but what we can say is that these large scales decay faster than the small scales or turbulence that is produced with small maximum scale. That is the only thing I can say about it at this point but that it is a really interesting topic. Actually, I think there are people here who may be able to answer your question better than I.

Roger Gaudreault Cascades Canada Inc

Did you change the crowding number in your experiments? What was the typical crowding number? What would be the effect of a change in crowding number on the floc rupture ratio?

Juha Salmela

Actually, I did not explain that figure very well. In the floc rupture ratio figure, I had all sorts of crowding numbers. Concentration was constant but all fibre properties changed. The floc rupture ratio seems to be somewhat empirical. Crowding number does not affect it and the length of the fibre is the dominant parameter. Crowding number itself is very important only when we have developing or fully developed pipe flow, but in the decaying turbulence field, this effect is more flow property than material property.

Ari Kiviranta

Please go back to your comment about the previous presentation and the question I asked, there. Did I understand correctly that what you are showing here is that the ratio between the step height and the fibre length has a big effect on deflocculation? So, if that ratio is too small, then you do not get proper deflocculation. That means that if you designed the headbox based on the short fibre furnish you always use in your trials and then you tried to use long fibres with that headbox, you would be in big trouble because it would not work. Does this mean that it will not deflocculate?

Juha Salmela

According to our study, it is as you suggest. What I am trying to say is that, first of all, we need to design flow geometries with specific fibre lengths in mind and, secondly, in the case of small scale turbulence, we need to be careful not to rely on measurements done with pure water.

Ari Kiviranta

Good, actually then I have another question here and it is about your figure number 3. You show the turbulence intensity and then also the floc volume and that actually quite early, after lets say 50–60 *mm* after the step, you have the minimum floc volume. In practical headboxes, you have quite a long distance from that point to the slice opening. What does that mean?

Discussion

Juha Salmela

It means that basically you are in trouble. If we could design a headbox that is just 50 *mm* long, we could get a very, very small floc size. It is now necessary to understand what is happening in a decaying turbulence field and what is happening in the boundary layers. This whole system is really interesting and demands a lot more research.

Jean-Claude Roux EFPG-INPG

I would like to bring to your attention an interesting point about your Figure 6. You are probably aware of it but I would like the audience also to consider it. Figure 6 implies that the floc rupture ratio has some limit when you increase the dimensionless step. This means that you have a limit of the technology of a one step diffuser. My question is what do you think of adding another step after this one? Can we avoid this limitation by including 2 or 3 steps?

Juha Salmela

We have done some experiments like that. The limiting floc size which we are approaching is actually very, very small and actually is close to the fibre size. My opinion is that we cannot go lower than that.

Jean-Claude Roux

I agree with your conclusion. It means that if we put two steps one after the other, the efficiency of the composite device has also some limitation?

Juha Salmela

Except that, with these extra steps, you postpone the position of the minimum floc size. So it goes further away from the step.

Jean-Claude Roux

If you start from a big floc volume you can still have further effects. If you are at the level in your experiments, it has little effect.